

# Langmuir–Blodgett Silver Nanowire Monolayers for Molecular Sensing Using Surface-Enhanced Raman Spectroscopy

Andrea Tao,<sup>†,||</sup> Franklin Kim,<sup>†,||</sup> Christian Hess,<sup>‡,||</sup> Joshua Goldberger,<sup>†</sup>  
Rongrui He,<sup>†</sup> Yugang Sun,<sup>§</sup> Younan Xia,<sup>§</sup> and Peidong Yang<sup>\*,†,‡</sup>

*Department of Chemistry, University of California, Berkeley, California 94720, Materials Science Division, Lawrence Berkeley National Laboratory, Berkeley, California 94720, and Department of Chemistry, University of Washington, Seattle, Washington 98195*

Received June 18, 2003; Revised Manuscript Received July 7, 2003

## ABSTRACT

Langmuir–Blodgett technique was used to assemble monolayers (with areas over 20 cm<sup>2</sup>) of aligned silver nanowires that are ~50 nm in diameter and 2–3 μm in length. These nanowires possess pentagonal cross-sections and pyramidal tips. They are close-packed and are aligned parallel to each other. The resulting nanowire monolayers serve as excellent substrates for surface-enhanced Raman spectroscopy (SERS) with large electromagnetic field enhancement factors ( $2 \times 10^5$  for thiol and 2,4-dinitrotoluene, and  $2 \times 10^9$  for Rhodamine 6G) and can readily be used in ultrasensitive, molecule-specific sensing utilizing vibrational signatures.

Significant progress has been made in the area of nanowire synthesis and device application in the past several years.<sup>1</sup> A grand challenge, however, still resides in the hierarchical organization of these nanoscale building blocks into functional assemblies and ultimately a useful system.<sup>2–5</sup> Successful alignment and patterning of nanowires would significantly impact many areas such as nanoscale electronics, optoelectronics, and molecular sensing. Previously, a microfluidic approach was used to align nanowires with limited success.<sup>3,4</sup> Langmuir–Blodgett (LB) assembly is a powerful technique that can be used to assemble a large-area monolayer of anisotropic building blocks.<sup>2,6,7</sup> Herein, we report our successful attempt to utilize this process to assemble aligned monolayers (with areas over 20 cm<sup>2</sup>) of silver nanowires that are ~50 nm in diameter and 2–3 μm in length. These nanowires (characterized by pentagonal cross-sections and pyramidal tips) can be close-packed as parallel arrays, with their longitudinal axes aligned perpendicular to the compression direction. The resulting nanowire monolayers can serve as good surface enhanced Raman spectroscopy (SERS) substrates, exhibit large electromagnetic field enhancement factors ( $2 \times 10^5$  for thiol and 2,4-dinitrotoluene,  $2 \times 10^9$  for Rhodamine 6G), and can readily be used in ultrasensitive, molecule-specific sensing utilizing vibrational signatures.

Silver nanowires were prepared using poly(vinyl pyrrolidone) (PVP) as the capping agent.<sup>8</sup> The as-prepared samples were purified to remove spherical nanoparticles. The resulting nanowires are uniform in both diameter ( $45.3 \pm 3.6$  nm) and aspect ratio ( $45 \pm 5$ ). After functionalizing with 1-hexadecanethiol ligands, the wires were rendered hydrophobic and redispersed in chloroform. Figure 1 shows a transmission electron microscopy image of the silver nanowires before the LB assembly. An important feature of these nanowires is their pentagonal cross-sections, as shown in the inset of Figure 1A. In addition, these wires possess pentagonal pyramidal ends with vertices as sharp as 2 nm (Figure 1B). The noncircular cross-sections and sharp wire tips might have important consequences for molecular sensing using surface enhanced Raman spectroscopy.<sup>9–12</sup> For a recent review on SERS, please refer to ref 13.

The nanowires were then dispersed onto a water surface of the Langmuir–Blodgett trough. It is important to note that the displacement of the PVP capping agents with thiol ligands is critical in rendering the nanowire surface hydrophobic as well as preventing aggregation. The assembly process is a microscopic version of “logs-on-a-river”. Figure 2A shows a photograph of the nanowires dispersed on the trough’s water surface. At this stage, the surface pressure is zero (see Figure 2D) and the nanowires are randomly oriented. The water surface is essentially transparent. When the nanowires were compressed, the surface pressure increased (Figure 2B,D). Above a certain critical surface pressure (14 mN/m), the monolayer underwent a Mott-

\* Corresponding author. E-mail: p\_yang@uclink.berkeley.edu.

† University of California.

‡ Lawrence Berkeley National Laboratory.

§ University of Washington.

|| These authors contributed equally to this work.

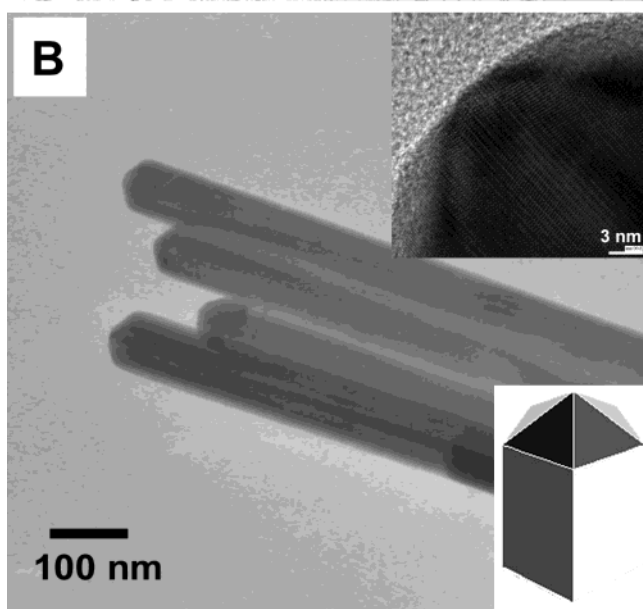
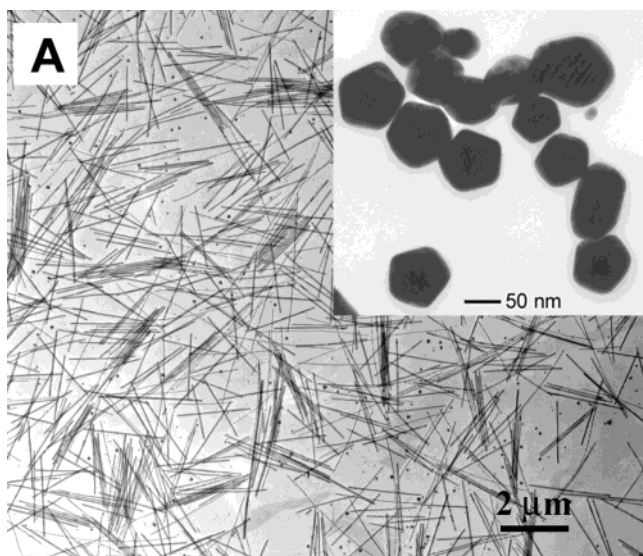


**Figure 1.** Transmission electron microscopy image of the uniform Ag nanowires. Inset in (A) is an image taken from a microtomed sample, showing the pentagonal cross-sections of the nanowires. The high-resolution TEM image, the upper inset in (B), shows the sharp pentagonal pyramidal tip of a silver nanowire, as schematically illustrated in the bottom inset (B).

insulator-to-metal transition, as previously seen in Langmuir–Blodgett monolayers of spherical Ag nanocrystals.<sup>14</sup> This transition is indicated by the appearance of a metallic sheen on the nanowire monolayer surface. Figure 2C shows the monolayer in its highly reflective metallic state. This particular sample covers a trough area of 20 cm<sup>2</sup>. However, this final aligned area is limited only by the amount of initial material used for the compression. We are able to prepare these monolayers on any substrate over an arbitrarily large area.

Most importantly, the compressed silver nanowire monolayer exhibits remarkable alignment parallel to the trough barrier. Figure 3 shows scanning electron microscopy (SEM) images of monolayer transferred onto a silicon wafer. The nanowires are aligned side-by-side over large areas, resem-

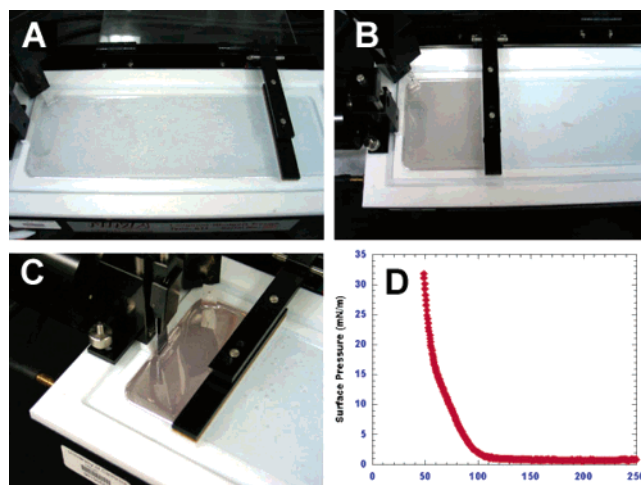


**Figure 2.** Langmuir–Blodgett (LB) nanowire assembly process. (A–C) Photographs of the nanowire assembly process at different compression stages. (D) Surface pressure curve recorded during the LB nanowire monolayer assembly.

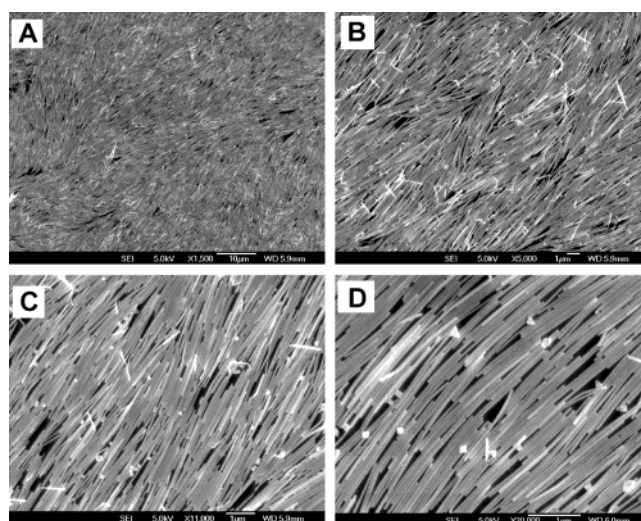


**Figure 3.** Scanning electron microscopy images (at different magnifications) of the silver nanowire monolayer deposited on a silicon wafer.

bling a nematic two-dimensional ordering of a liquid crystal. This large-scale directional ordering was also verified by imaging the sample under an optical microscope equipped with a cross-polarizer (see Supporting Information). The aligned nanowire domains displayed alternating extinction patterns when the sample was rotated every 45 degrees.

The dependence of the extinction spectra as a function of the polarization angle of the input optical beam was recorded with a polarized UV–vis spectrometer. Figure 4 shows a typical set of UV–vis spectra at different polarization angles. Strong optical dichroism can be seen in these spectra. Three sets of peaks were observed: 350 nm, 380 nm, and a broad peak at 500–700 nm. When the polarization of the incident light is perpendicular to the wire axis, the transverse mode of the surface plasmons experiences preferred excitation; as a result, the 380 nm extinction peak exhibits the highest intensity with this configuration. When the polarization angle

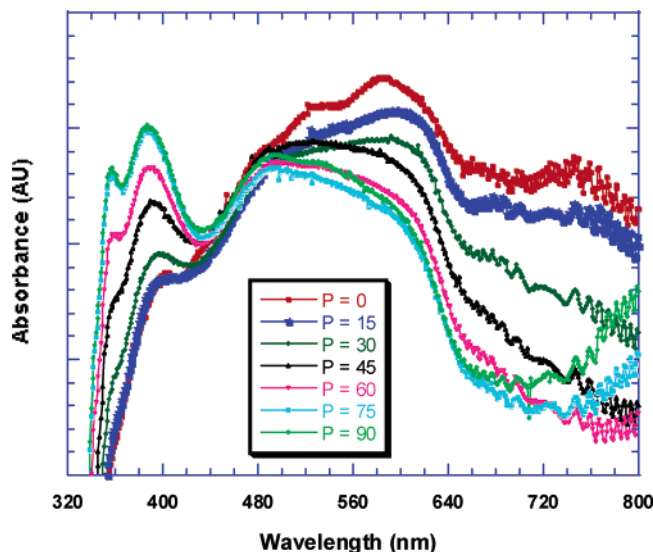


**Figure 4.** UV-vis absorption spectra of the silver nanowire monolayer. All spectra were obtained at normal incidence with the polarization angles ( $P$ ) defined as  $\theta = 0^\circ$ , when the incident electric field is parallel to the direction of nanowire alignment and  $\theta = 90^\circ$  when the field is perpendicular to the nanowire axis.

was increased from  $0^\circ$  (normal to wire axis) to  $90^\circ$  (parallel to wire axis), the intensity for the 500–600 nm peaks increased. This extinction peak can be attributed to the excitation of longitudinal plasmons within the monolayer.<sup>15</sup> The significant broadening is believed to stem from the coupling of electromagnetic waves among neighboring nanowires.<sup>16,17</sup>

This large area of nanowire alignment demonstrated here would enable the fabrication of high-density nanoscale interconnects,<sup>5</sup> sensor arrays, as well as multilayer structures via a layer-by-layer transfer approach. These monolayers can be readily transferred to any desired substrate, including silicon wafers, glass slides, and polymer substrates. For example, we have successfully embedded monolayers and multilayers of these silver nanowires within poly(dimethylsiloxane) (PDMS), giving flexible nanowire-polymer composites that can serve as simple wire-grid optical polarizers. Thus, this Langmuir-Blodgett approach is a very powerful technique for the organization of anisotropic building blocks into functional nanoscale assemblies with unprecedentedly high packing density.

Significantly, these aligned nanowire monolayers can be readily used as surface-enhanced Raman spectroscopy (SERS) substrates for molecular sensing with high sensitivity and specificity. These metallic layers are expected to exhibit giant local electromagnetic (EM) field enhancement, particularly for nanowires with sharp tips and noncircular cross-sections (as in the current case, a pentagonal cross-section).<sup>9–12</sup> Figure 5A shows the SERS spectrum of 1-hexadecanethiol on a Langmuir-Blodgett film of silver nanowires for visible (532 nm, 25 mW) and near-infrared excitation (785 nm, 10 mW). The observed bands were characteristic of 1-hexadecanethiol.<sup>18,19</sup> The Raman bands in the low-frequency part of the spectrum include the  $\nu(\text{C}-\text{S})_{\text{trans}}$  at  $701 \text{ cm}^{-1}$ ; the  $\text{CH}_3$  rocking mode at  $891 \text{ cm}^{-1}$ ; the

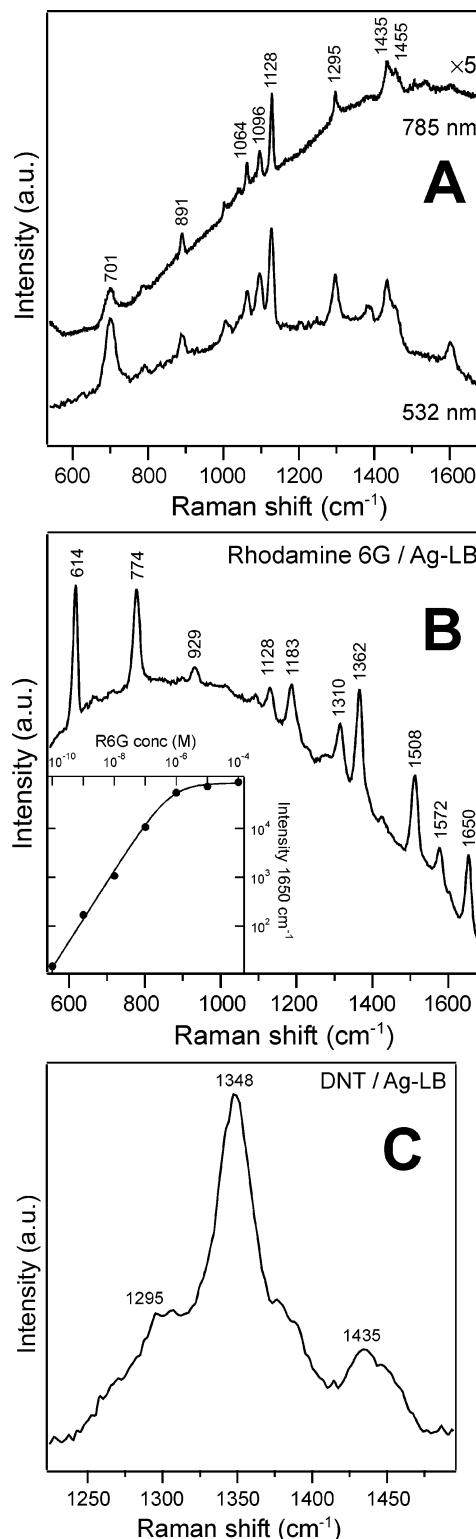


**Figure 5.** Surface-enhanced Raman spectroscopy on the silver nanowire monolayer. (A) SERS spectra of 1-hexadecanethiol on a Langmuir-Blodgett film of silver nanowires with visible (532 nm, 25 mW) and near-infrared excitation (785 nm, 10 mW). (B) SERS spectrum of R6G on the thiol-capped Ag-LB film (532 nm, 25 mW) after 10 min incubation in a  $10^{-9}$  M R6G solution. The inset shows the linear relationship between the Raman intensity at  $1650 \text{ cm}^{-1}$  and the R6G concentration. (C) SERS spectrum of 2,4-DNT on the thiol-capped Ag nanowire monolayers after incubation for 10 min in  $10^{-2}$  M 2,4-DNT/MeOH solution. The spectrum was recorded using 25 mW of 532 nm laser light. The acquisition time was 10 s.

$\nu(\text{C}-\text{C})$  at 1064, 1096, and 1128  $\text{cm}^{-1}$ ; the  $\text{CH}_2$  wag at 1295  $\text{cm}^{-1}$ ; the  $\text{CH}_2$  twist at 1435  $\text{cm}^{-1}$ ; and the  $\text{CH}_2$  scissor at 1455  $\text{cm}^{-1}$ . The  $\nu(\text{C}-\text{S})_{\text{trans}}$  at 701  $\text{cm}^{-1}$  is indicative of well-ordered alkyl chains with largely trans conformation near the thiol headgroup.<sup>20</sup> In the C–C region, the presence of an intense 1128  $\text{cm}^{-1}$  and a weaker 1096  $\text{cm}^{-1}$  neighbor (indicative of trans bonding) suggests that the adsorbed thiol possesses a “solidlike” structure extending beyond the surface region into the hydrocarbon tail.

The enhancement factor (EF) for 1-hexadecanethiol/Ag was calculated according to the following expression:<sup>21</sup>

$$\text{EF} = [I_{\text{SERS}}]/[I_{\text{Raman}}] \times [M_{\text{b}}]/[M_{\text{ads}}]$$

where  $M_{\text{b}}$  is the concentration of molecules in the bulk sample and  $M_{\text{ads}}$  is the concentration of adsorbed molecules.  $I_{\text{SERS}}$  and  $I_{\text{Raman}}$  are intensities in the SER and Raman spectrum, respectively. The concentration of adsorbed molecules was estimated by dividing the total surface area of a single nanowire by the van der Waals dimensions ( $2.3 \text{ \AA} \times 2.3 \text{ \AA}$ ) of the thiol headgroup. Assuming 1-hexadecanethiol forms a close-packed monolayer perpendicular to the surface, the number of adsorbed molecules was calculated to be  $2.5 \times 10^{14}/\text{cm}^2$ . Intensities were compared to the Raman scattering of a 0.1 M 1-hexadecanethiol solution. For the vibrational mode at 1295  $\text{cm}^{-1}$ , an EF of  $2 \times 10^5$  was obtained. Values of similar magnitude have been observed on other SERS-active Ag substrates at optimum visible excitation wavelengths. This enhancement can be attributed to increased local optical fields near the Ag surface due to the excitation of surface plasmon resonances.

Interestingly, near-infrared excitation (785 nm) of 1-hexadecanethiol/Ag gave rise to comparable SERS intensities. We believe this effect stems from the interaction of individual Ag wires within the film. In the absorption spectrum of an LB film, a broad resonance evolves from this interaction, giving a peak around 550 nm that extends into the near-infrared region. Thus, LB nanowire films should serve as extremely versatile SERS substrates, allowing excitation over a wide range of frequencies.

Rhodamine 6G (R6G) is a strongly fluorescent xanthen derivative which shows a molecular resonance Raman (RR) effect when excited at 532 nm. Figure 5B depicts the SERRS spectrum of R6G on a thiol-covered LB film after a 10-minute incubation in a  $10^{-9}$  M R6G solution. A detailed assignment of the spectral features has been reported previously and will not be repeated here.<sup>22</sup> The quenching of the fluorescence and huge SERRS enhancement factor indicate that the R6G molecules spontaneously adsorb on the Ag nanowires. In addition, a linear relationship between the intensity of band at 1650  $\text{cm}^{-1}$  and the R6G concentration was observed (Figure 5B, inset). A least-square fit of the data (solid line in inset) using a Langmuir adsorption isotherm gives an adsorption energy of 46 kJ/mol, which suggests that R6G has strong interaction with the surface of the wires.<sup>22</sup> More importantly, these observations show that despite the presence of thiol capping agents, the surface of the Ag nanowire film offers free sites which allow for the

adsorption and therefore identification of any unknown analyte. Based on the field enhancement factor obtained for the thiol and the fact that the ratio of the Raman intensities of the R6G- and thiol-related C–C stretching bands at R6G saturation coverage is  $\sim 10^4$ , the EF for R6G is estimated to be  $2 \times 10^9$ .

The observed large enhancement factors suggest that these monolayers can indeed serve as robust solid substrates for carrying out molecular sensing with high sensitivity and specificity (as SERS readily reveals the vibrational signature of an analyte). Here we demonstrate the capability of our nanowire substrates for the detection of 2,4-dinitrotoluene (2,4-DNT), the most common nitroaromatic compound for detecting buried landmines and other explosives.<sup>23</sup> SERS from 2,4-DNT has been obtained previously.<sup>24</sup> Figure 5C shows a SERS spectrum of 2,4-DNT adsorbed on the thiol-capped Ag nanowire monolayers. The  $\text{NO}_2$  stretching mode at 1348  $\text{cm}^{-1}$ —the key vibrational mode for the analysis of 2,4-DNT—is clearly displayed and well-separated from the surfactant-related Raman bands at 1295 and 1435  $\text{cm}^{-1}$ . We achieve a sensitivity of approximately 0.7 pg, assuming a monolayer coverage for 2,4-DNT and an area of 45  $\text{\AA}^2$  per adsorbate. Based on the same assumptions, an EF of  $2 \times 10^5$  was calculated for the vibration mode at 1348  $\text{cm}^{-1}$ .

Although comparable sensitivities and EF values have been reported for colloidal Au and Ag, as well as roughened metal surfaces,<sup>13</sup> the use of our nanowire monolayers as SERS substrates has several advantages. First, the surface properties of these nanowire monolayers are highly reproducible and well-defined as compared to other systems.<sup>25</sup> Second, the unique features of the nanowires (sharp vertices, noncircular pentagonal cross-sections, interwire coupling) may lead to larger field enhancement factors, offering higher sensitivity under optimal conditions.<sup>9–11</sup> In addition, strong wire coupling within the monolayers enables SERS experiments with a broad selection of excitation sources. Last, these monolayers can readily be used for molecular detection in either an air-borne or a solution environment. Hence, our nanowire-based sensing scheme could have significant implications in chemical and biological warfare detection, national and global security, as well as medical detection applications.

**Acknowledgment.** This work was supported in part by the Camille and Henry Dreyfus Foundation, ACS-Petroleum Research Fund, the Alfred P. Sloan Foundation, the Hellman Family Faculty Foundation, the Beckman Foundation, the David and Lucile Packard Foundation, the Department of Energy, the National Science Foundation, and the AFOSR-MURI program. C.H. thanks the Max-Planck Society for a fellowship. A. T. thanks the National Science Foundation for a graduate fellowship. Work at the Lawrence Berkeley National Laboratory was supported by the Office of Science, Basic Energy Sciences, Division of Materials Science of the U.S. Department of Energy. We thank the National Center for Electron Microscopy for the use of their facilities. We thank Prof. Alex Bell and Renishaw Inc. for allowing us to use their Raman spectrometers.

**Supporting Information Available:** Details for materials synthesis and characterization methodologies. This material is available free of charge via the Internet at <http://pubs.acs.org>.

## References

- (1) Xia, Y.; Yang P.; Eds. Special issue on one-dimensional nanostructures. *Adv. Mater.* **2003**, *15*(5).
- (2) Kim, F.; Kwan, S.; Arkana, J.; Yang, P. *J. Am. Chem. Soc.* **2001**, *123*, 4386.
- (3) Messer, B.; Song, J. H.; Yang, P. *J. Am. Chem. Soc.* **2000**, *122*, 10232.
- (4) Huang, Y.; Duan, X. F.; Wei, Q.; Lieber, C. M. *Science* **2001**, *291*, 630.
- (5) Melosh, N. A.; Boukai, A.; Diana, F.; Gerardot, B.; Badolato, A.; Petroff, P. M.; Heath, J. R. *Science* **2003**, *300*, 112.
- (6) Kwan, S.; Kim, F.; Arkana, J.; Yang, P. *Chem. Commun.* **2001**, *5*, 447.
- (7) Chung, S. W.; Markovich, G.; Heath, J. R. *J. Phys. Chem. B* **1998**, *102*, 6685.
- (8) Sun, Y. G.; Gates, B.; Mayers, B.; Xia, Y. N. *Nano Lett.* **2002**, *2*, 165.
- (9) Kottmann, J. P.; Martin, O. J.; Smith, D. R.; Schultz, S. *Phys. Rev. B* **2001**, *64*, 235402.
- (10) Kottmann, J. P.; Martin, O. J.; Smith, D. R.; Schultz, S. *Chem. Phys. Lett.* **2001**, *341*, 1.
- (11) Kottmann, J. P.; Martin, O. J. *Optics Exp.* **2001**, *8*, 655.
- (12) Garcia-Vidal, F. J.; Pendry, J. B. *Phys. Rev. Lett.* **1996**, *77*, 1163.
- (13) Kneipp, K.; Kneipp, H.; Itzkan, I.; Dasari, R. R.; Feld, M. S. *J. Phys.: Condens. Matter* **2002**, *14*, R597 and references therein.
- (14) Heath, J. R.; Knobler, C. M.; Leff, D. V. *J. Phys. Chem. B* **1997**, *101*, 189.
- (15) Al-Rawashdeh, N. A. F. *J. Phys. Chem. B* **1998**, *102*, 361.
- (16) Zhao, L.; Kelly, K. L.; Schatz, G. C. *J. Phys. Chem. B* **2003**, *107*, 668.
- (17) Gotschy, W.; Vonmetz, K.; Leitner, A.; Aussenegg, F. R. *Optics Lett.* **1996**, *21*, 1099.
- (18) Bercegol, H.; Boerio, F. J. *Langmuir* **1994**, *10*, 3684.
- (19) Garoff, S.; Sandroff, C. J. *J. Phys. Colloq.* **1983**, C10, *44*, 483.
- (20) Schoenfish, M. H.; Pemberton, J. E. *J. Am. Chem. Soc.* **1998**, *120*, 4502.
- (21) Nokoobakht, B.; Wang, J.; El-Sayed, M. A. *Chem. Phys. Lett.* **2002**, *366*, 17.
- (22) Hildebrandt, P.; Stockburger, M. *J. Phys. Chem.* **1984**, *88*, 5935.
- (23) McHugh, C. J.; Keir, R.; Graham, D.; Smith, W. E. *Chem. Commun.* **2002**, 580.
- (24) Sylvia, J. M.; Janni, J. A.; Klein, J. D.; Spencer, K. M. *Anal. Chem.* **2000**, *72*, 5834.
- (25) Steinfeld, J. I.; Wormhoudt, J. *Annu. Rev. Phys. Chem.* **1998**, *49*, 203.

NL0344209